

We are IntechOpen, the world's leading publisher of Open Access books Built by scientists, for scientists

6,900

Open access books available

185,000

International authors and editors

200M

Downloads

Our authors are among the

154

Countries delivered to

TOP 1%

most cited scientists

12.2%

Contributors from top 500 universities



WEB OF SCIENCE™

Selection of our books indexed in the Book Citation Index
in Web of Science™ Core Collection (BKCI)

Interested in publishing with us?
Contact book.department@intechopen.com

Numbers displayed above are based on latest data collected.
For more information visit www.intechopen.com



Analysis of Compensated Six-Phase Self-Excited Induction Generator Using Double Mixed State-Space Variable Dynamic Model

Kiran Singh

Abstract

In this article, a mixed current-flux d-q modeling of a saturated compensated six-phase self-excited induction generator (SP-SEIG) is adopted during the analysis. Modeling equations include two independent variables namely stator current and magnetizing flux rather than single independent variables either current or flux. Mixed modeling with stator current and magnetizing flux is simple by having only four saturation elements and beneficial in study of both stator and rotor parameters. Performance equations for the given machine utilize the steady-state saturated magnetizing inductance (L_m) and dynamic inductance (L). Validation of the analytical approach was in good agreement along with three-phase resistive or resistive-inductive loading and also determined the relevant improvement in voltage regulation of machine using series capacitor compensation schemes.

Keywords: mixed double state space variables, self-excitation, six-phase, compensation, induction generator, non-conventional energy

1. Introduction

Traditionally, synchronous generators have been used for power generation, but induction generators are increasingly being used these days because of their relative advantageous features over conventional synchronous generators. The need for external reactive power limits the application of an induction generator as isolated unit. The use of SEIG, due to its reduced unit cost, simplicity in operation and ease of maintenance are most suited in such system. These entire features facilitate the operation of induction generator in stand-alone mode to supply far-flung areas where extension of grid is economically not viable. The stand-alone SEIG can be used with conventional as well as non-conventional energy sources to feed remote single family, village community, etc. in order to expedite the electrification of rural and remote locations. A detailed dynamic performance of induction generator 'IG' operating in different modes i.e. isolated and grid-connected is necessary for the optimum utilization of its various favorable features. The investigations spread over last two decades also indicate the technical and economic vitality of using number

of phases higher than three in AC machines for applications in marine ships, thermal power plant to drive induced draft fans, electric vehicles and circulation pumps in nuclear power plants etc. In this area, research is still in its early stage, yet some extremely great authority's findings have been reported in the previous literatures indicating the general expediency of multi-phase systems. The literature regarding multi-phase IG is nearly not available since it has only three findings before 2004. The first article on multi-phase induction generator is appeared in 2005, along with rest of theoretical and practical works on SP-SEIG using single state- space variables either stator and rotor d-q axis currents or stator and rotor d-q axis flux linkages so far as reported [1]. On the basis of previous article reviews, before companion paper of 2015 [1], there were no literatures on modeling and analysis of SP-SEIG, using d-q axis components of stator current and magnetizing flux as mixed state-space variables. In the view of novelty, such mathematical modeling and analysis were carried out in detail for three-phase SEIG only, in a very few available literatures and some of which are mentioned by [2]. The purpose of this article is also to accomplish a similar task for modeling and analysis of SP-SEIG with series compensation scheme using double state-space variables as were proposed by companion paper without compensation. The simulation is performed on series compensated SP-SEIG by using 4th order Runge-Kutta subroutine in Matlab software.

2. Modeling description

Concerns about mathematical modeling of SP-SEIG, short-shunt series compensation capacitors and static resistive 'R' and balanced three-phase reactive 'R-L'

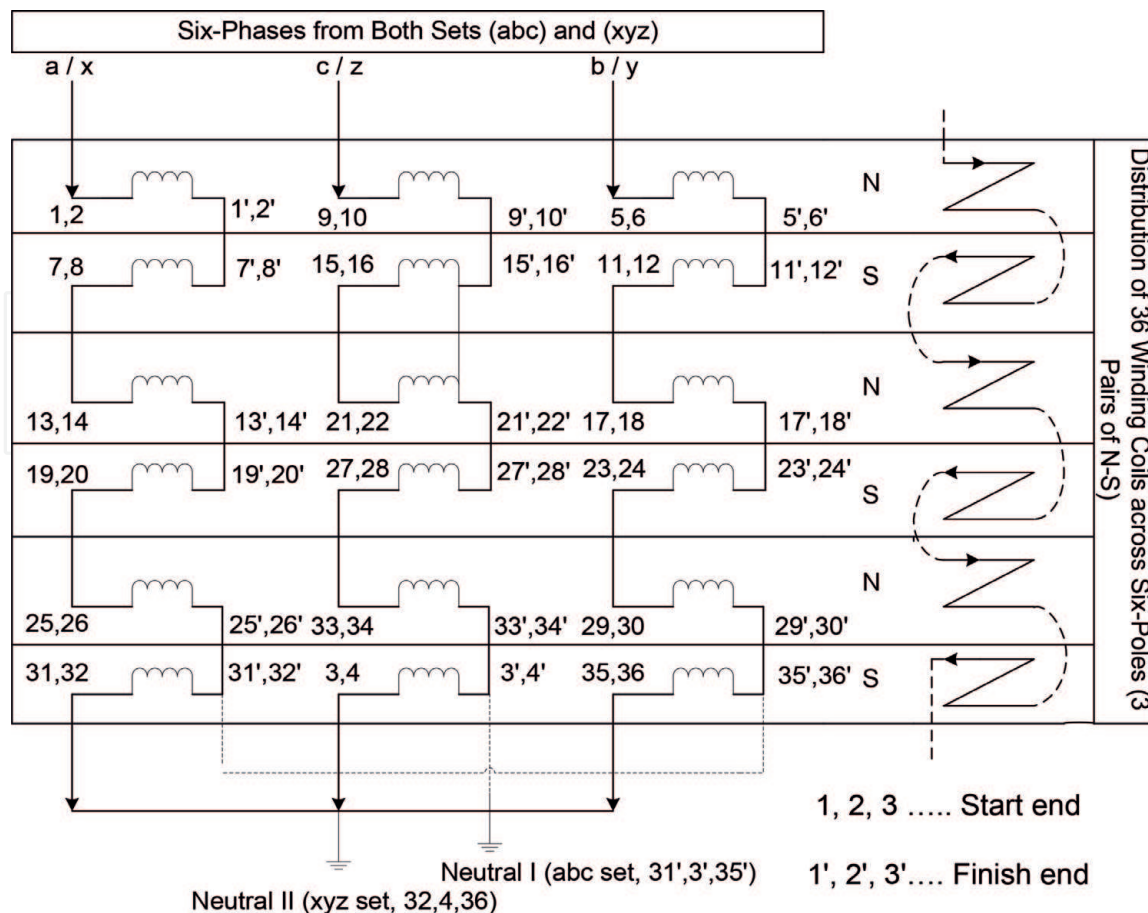


Figure 1. Distribution of 6-phases in 36 slots of 6 pole induction machine.

loads as previously discussed in [1, 3] are not described in this section, only briefly summarized along with newly addition of long-shunt series compensation capacitors.

2.1 SP-SEIG model

A basic two-pole, six-phase induction machine is schematically described by its stator and rotor axis [1]. In which, six stator phases of both sets, a, b, c and x, y, z (set I and II, respectively) are arranged to form two sets of uniformly distributed star configuration, displaced by an arbitrary angle of 30 electrical degree gravitate asymmetrical winding structure. The distribution of 6-phases in 36 slots of 6 pole induction machine is also shown in **Figure 1**. Previously, voltage equations using single state-space variable namely flux linkage were used in the expanded form for six-phase induction machine.

After simplification of voltage equations using double mixed state-space variables namely stator currents and magnetizing fluxes in the machine model following form occurs from Eqs. (1)–(39) of [1]:

$$[V_{dq}] = [H][dX_{dq}]/dt + [J][X_{dq}] \quad (1)$$

where $[V_{dq}] = [V_{d1} V_{q1} V_{d2} V_{q2} 0 0]^t$, $[X_{dq}] = [i_{d1} i_{q1} i_{d2} i_{q2} \Psi_{dm} \Psi_{qm}]^t$ and matrices $[H]$ and $[J]$ are given by Eqs. (2) and (3), respectively.

$$7 \begin{bmatrix} -L_{\sigma 1} & 0 & 0 & 0 & 1 & 0 \\ 0 & -L_{\sigma 1} & 0 & 0 & 0 & 1 \\ 0 & 0 & -L_{\sigma 2} & 0 & 1 & 0 \\ 0 & 0 & 0 & -L_{\sigma 2} & 0 & 1 \\ L'_{\sigma r} & 0 & L'_{\sigma r} & 0 & \left(1 + \frac{L'_{\sigma r}}{L'_{dd}}\right) & \frac{L'_{\sigma r}}{L_{dq}} \\ 0 & L'_{\sigma r} & 0 & L'_{\sigma r} & \frac{L'_{\sigma r}}{L_{dq}} & \left(1 + \frac{L'_{\sigma r}}{L_{qq}}\right) \end{bmatrix} \quad (2)$$

$$\begin{bmatrix} -r_1 & wL_{\sigma 1} & 0 & 0 & 0 & -w \\ -wL_{\sigma 1} & -r_1 & 0 & 0 & w & 0 \\ 0 & 0 & -r_2 & wL_{\sigma 2} & 0 & -w \\ 0 & 0 & -wL_{\sigma 2} & -r_2 & w & 0 \\ r'_r & -(w - w_r)L'_{\sigma r} & r'_r & -(w - w_r)L'_{\sigma r} & \frac{r'_r}{L_m} & -(w - w_r)\left(1 + \frac{L'_{\sigma r}}{L_m}\right) \\ (w - w_r)L'_{\sigma r} & r'_r & (w - w_r)L'_{\sigma r} & r'_r & -(w - w_r)\left(1 + \frac{L'_{\sigma r}}{L_m}\right) & \frac{r'_r}{L_m} \end{bmatrix} \quad (3)$$

The nonlinear equations of voltage and current across the shunt excitation capacitor and series compensation capacitors (short-shunt and long-shunt) can be transformed into d-q axis by using reference frame theory, i.e. Park's (d_{q0}) transformation [4], are given by Section 2.2 of [1] and (Section 2.3 of [1] and by following Section 2.2), respectively. Modeling of static loads is also given in Section 3 of [1].

2.2 Modeling of long-shunt capacitors

Current through series capacitors C_{ls1} and C_{ls2} (in case of long shunt), connected in series with winding set I and II, respectively, is same as the machine

$\Psi_{dm}, \Psi_{qm}, 1/L_{dd}, 1/L_{dq}, 1/L_{dq}$	d- and q-axis magnetizing flux linkages, saturation dependent coefficients of system matrix A
$p, \sigma, P, J, \theta_r, \omega, \omega_b, \omega_r$	differentiation w. r. t. time, index for constant, number of pole pairs, moment of inertia, electrical angular displacement of the rotor, reference frame speed, base speed and rotor speed
$L_m, L, L_{dq}, \cos\mu, \sin\mu$	steady-state saturated magnetizing inductance, dynamic inductance, cross-saturation coupling between the d- and q-axis of stator, angular displacements of the magnetizing current space vector with respect to the d-axis of the common reference frame
$C_{ls1} C_{ls2}$	long-shunt capacitors across the stator winding set I and II

Table 1.
Machine model symbols.

current. The machine current along with series capacitance determine the voltage across series long-shunt capacitor and when transformed in to d-q axis by using Park's transformation is given in Eqs. (4) and (5) [5–7].

$$\begin{aligned}
 \rho V_{q1s} &= i_{q1}/C_{ls1} \\
 \rho V_{d1s} &= i_{d1}/C_{ls1} \\
 \rho V_{q2s} &= i_{q2}/C_{ls2} \\
 \rho V_{d2s} &= i_{d2}/C_{ls2}
 \end{aligned} \tag{4}$$

and the load terminal voltage is expressed as

$$\begin{aligned}
 V_{Lq1} &= V_{q1} + V_{q1s} \\
 V_{Ld1} &= V_{d1} + V_{d1s} \\
 V_{Lq2} &= V_{q2} + V_{q2s} \\
 V_{Ld2} &= V_{d2} + V_{d2s}
 \end{aligned} \tag{5}$$

The remaining symbols of machine model have their usual meanings from Ref. [1] and **Table 1**.

3. Methodology

In this section, a numerical method is introduced to the solution of Eqs. (1)–(3); where double mixed current flux state space model is discussed by [1]. The ordinary linear differential equations can be solved by the analytical technique rather than approximation method. Eq. (1) is non-linear differential and cannot be solved exactly with high expectations, only approximations are estimated numerically by computer technique using 4th order Runge-Kutta method or classical Runge-Kutta method or often referred as “RK4” as so commonly used [8]. The analytical response of compensated SP-SEIG in only single operating mode is carried out under significant configuration using RK4 subroutine implemented in Matlab M-file. The dynamic performances were determined under no load, R load and R-L loading condition in only the single mode of excitation capacitor bank, and in both modes of compensating series capacitor bank. The following analytical dynamic responses of series compensated SP-SEIG is considered for the validity of proposed approaches in this chapter.

- During R and R-L loading with short shunt compensation.
- During R and R-L loading with long shunt compensation.

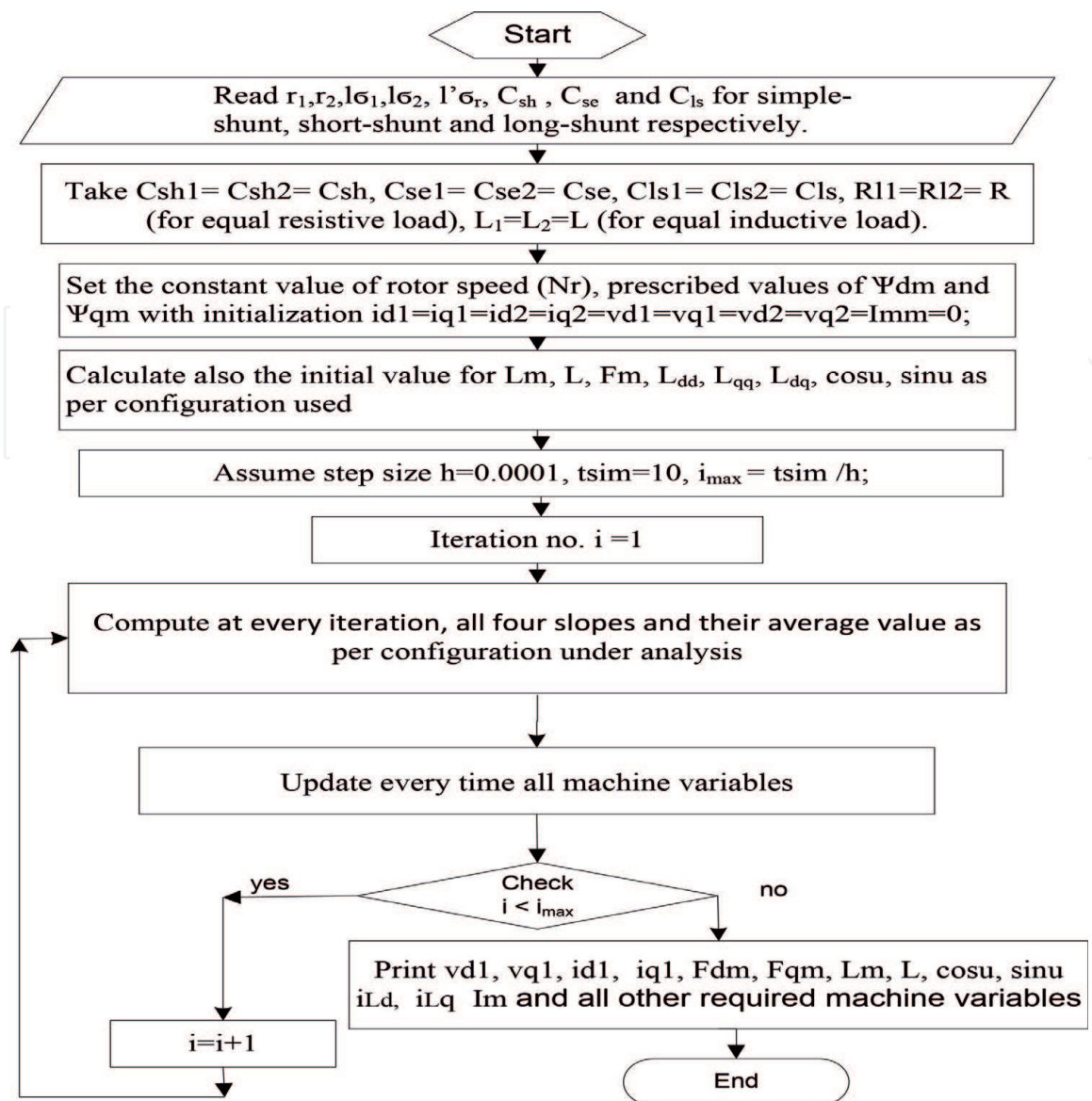


Figure 2. Algorithm for Runge-Kutta method implemented for SP-SEIG under constant rated speed at 1000 RPM.

Both analytical responses are well detailed in Section 4. The analytical study of compensated SP-SEIG is given in Section 4 by using an explicit MATLAB program incorporates the RK4 method. An Algorithm of RK4 method for the analysis of compensated SP-SEIG is also shown in **Figure 2**. The parameters of studied machine and saturation dependent coefficients of system matrix [H] are also reported by [1] for further dynamic analysis of saturated compensated SP-SEIG using double mixed state space variable model under constant rotor speed along with appropriate initial estimated variables values which are also responsible in the development of rated machine terminal voltage and it depends on other machine variables.

4. Analytical response

Analytical performances of compensated SP-SEIG are illustrated in **Figures 3–6** along with sudden switching of R load of 200 Ω and a balanced three-phase R-L load (200 Ω in series with 500 mH) at t = 2 s when short-shunt and long-shunt compensation along both three-phase winding sets. These waveforms are

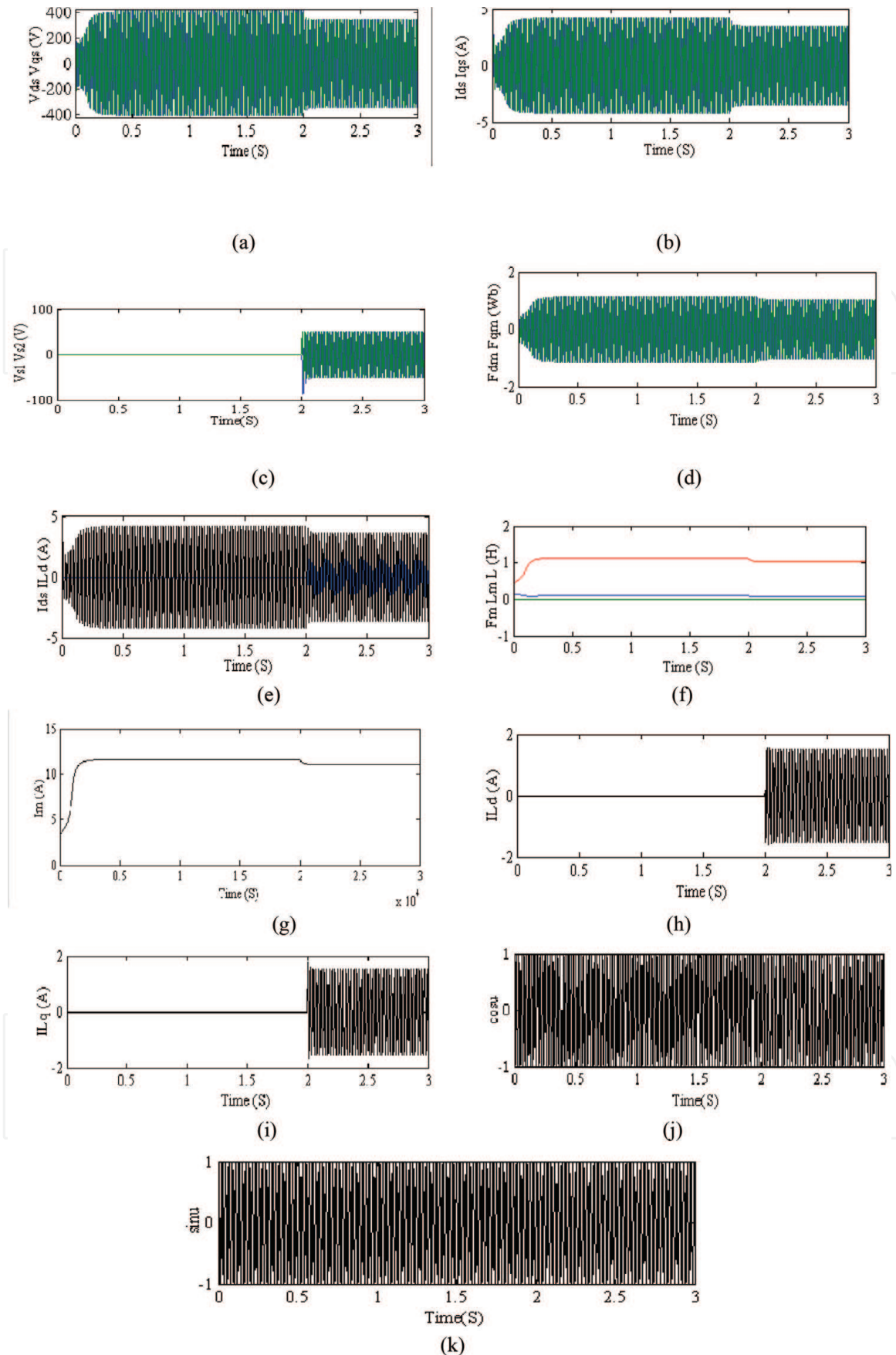


Figure 3. Analytical waveforms during sudden switching of R load of 200 Ω at $t = 2$ s.

correspond to d-q axis stator voltage, d-q axis stator current, d-q axis load current, d-q axis magnetizing flux, d-q axis series capacitor voltage and magnetizing current. In the case of R-L load, generated voltage and current amplitude has been dropped few more volts and amperes, respectively, compared to R load. Combined

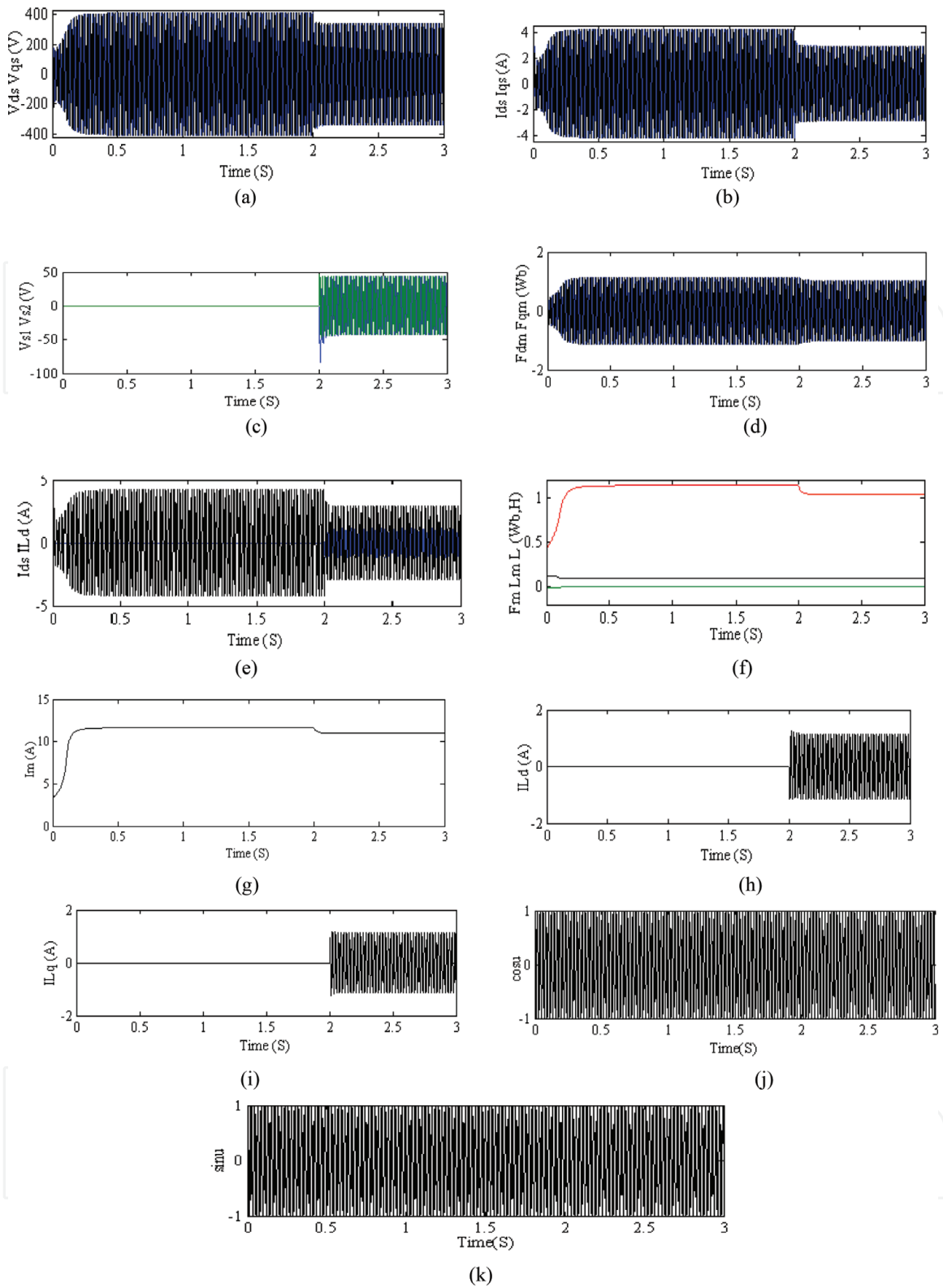


Figure 4.
 Analytical waveforms during sudden switching of RL load at $t = 2$ s.

amplitude of magnetizing flux, steady-state saturated magnetizing inductance and dynamic (tangent slope) inductance along with the combined amplitude waveform of d-axis stator current and load current during no-load and sudden switching of R load of 200Ω at $t = 2$ s are also shown in **Figures 3–6**. As per discussion of [1], generated RMS value of steady state terminal voltage and current is about 225 V line to line and 4.46 A at rated speed of 1000 RPM with the value of excitation capacitance of $38.5 \mu\text{F}$ per phase in simple-shunt configuration for the selected machine in this article. In proposing stator current and magnetizing flux mixed variable model,

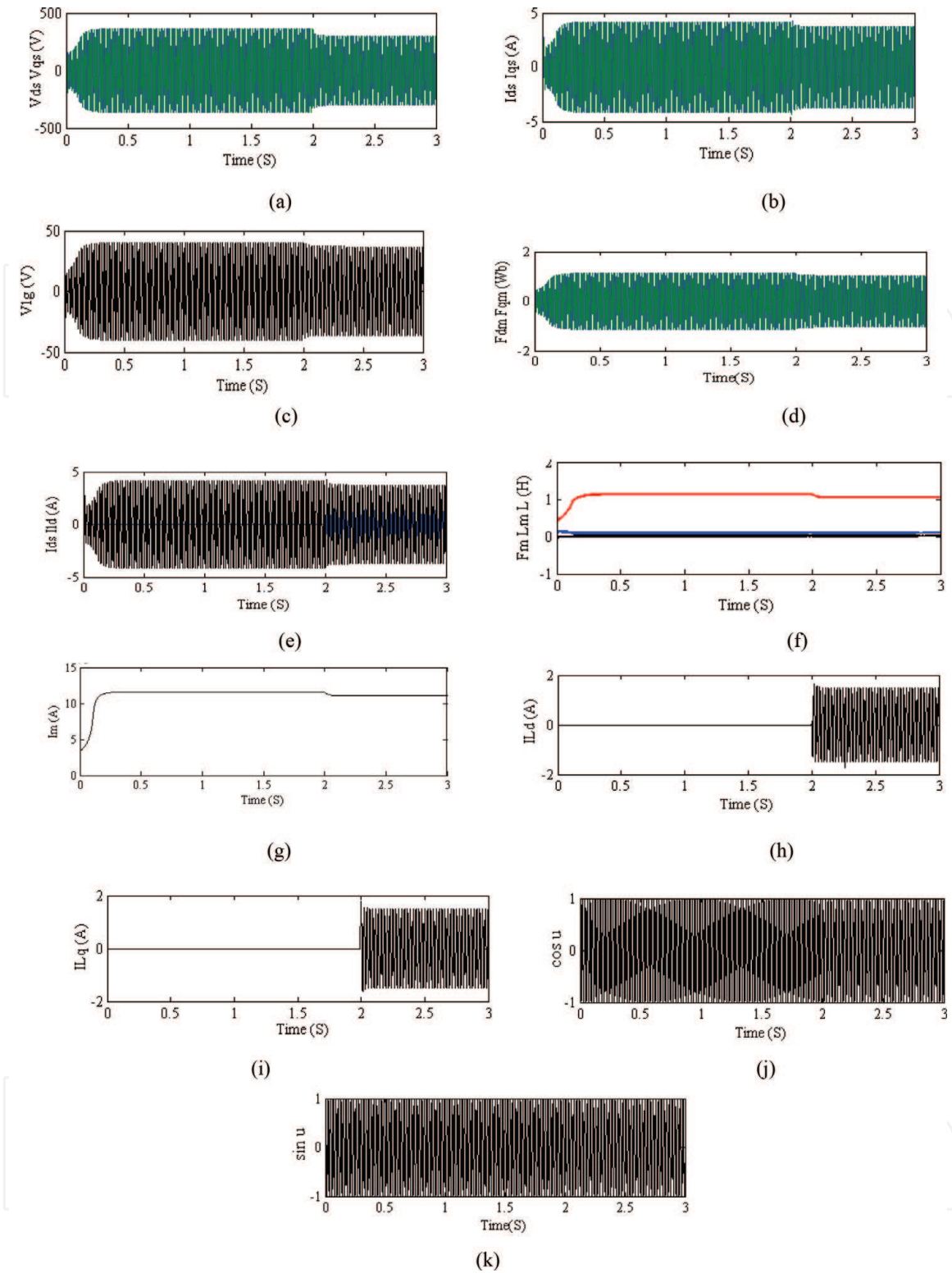


Figure 5.
Analytical waveforms during sudden switching of R load of 200Ω at $t = 2 \text{ s}$.

it has been observed that SP-SEIG terminal voltage and current build-up from their initial values to final steady state values entirely depends upon its initial few Weber values of d- and q-axis magnetizing flux at constant rated speed of 1000 RPM.

4.1 Short-shunt series compensated SP-SEIG

Performance of short-shunt SP-SEIG in only its single mode of operation using the values of excitation and series capacitor banks of 38.5 and $108 \mu\text{F}$ per phase, respectively, has been predicted from the built explicit MATLAB program using RK4 subroutine. Computed waveforms are shown in **Figures 3 and 4**. Application

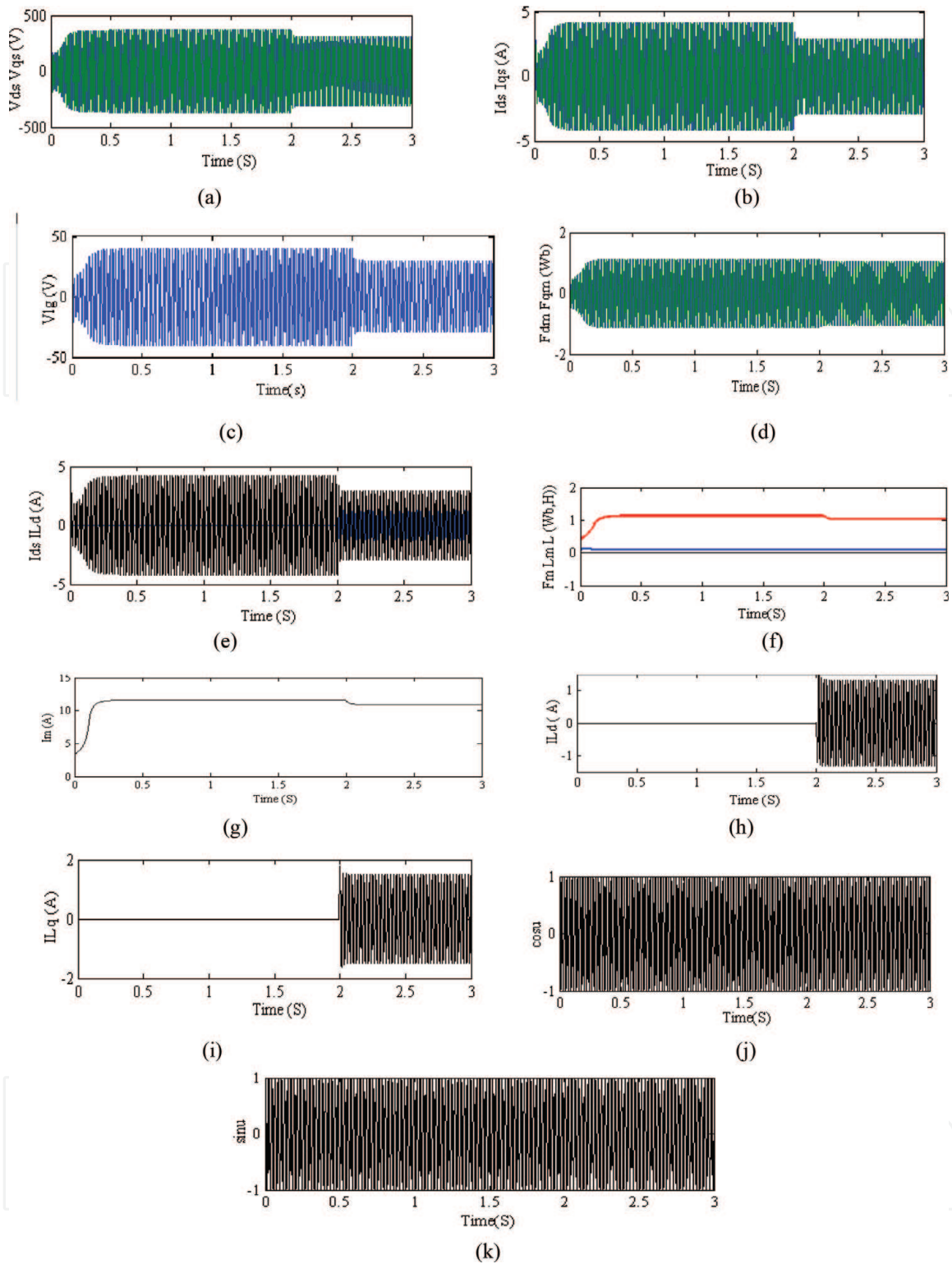


Figure 6.
 Analytical waveforms during sudden switching of R-L load at $t = 2$ s.

of short-shunt scheme results in overvoltage across the generator terminals as shown in **Figure 3a**, the per phase voltage level is more than the voltage level of **Figure 5a** and it is illustrated in **Figure 3c**.

4.1.1 When both three-phase winding sets are connected in short-shunt configuration with independent R loading

The analytical d-q waveform of voltage, current, magnetizing flux and magnetizing current during no-load and sudden switching of R load of 200Ω at $t = 2$ s are shown in corresponding **Figure 3a, b, d** and **g**. In addition, combined amplitude

waveforms of magnetizing flux, steady-state saturated magnetizing inductance and dynamic (tangent slope) inductance is shown in **Figure 3f**. The angular displacements of the magnetizing current space vector with respect to the d-axis of the common reference frame are also shown in **Figures 3j** and **k**. The combined d-q axis voltage drop across the series short-shunt capacitor is given in **Figure 3c** and combined amplitude waveform of d-axis stator current and load current during no-load and sudden switching of R load of $200\ \Omega$ at $t = 2\ \text{s}$ is given in **Figure 3e**. The d- and q-axis load currents are also depicted in **Figure 3h** and **i**, respectively, during sudden switching of R load of $200\ \Omega$ at $t = 2\ \text{s}$.

4.1.2 When both three-phase winding sets are connected in short-shunt configuration with independent R-L loading

In the same order of figure numbers, all computed waveforms are shown in **Figure 4** with sudden switching of R-L load ($200\ \Omega$ resistance in series with $500\ \text{mH}$ inductor) at $t = 2\ \text{s}$. Analytical generated RMS steady state voltage and corresponding current at rated speed of $1000\ \text{RPM}$ are shown in **Figure 4a** and **b**. Drops in d-q-axis generating and lagging load currents are shown in **Figure 4b, h** and **i**.

4.2 Long-shunt series compensated SP-SEIG

It is also seen that like short-shunt compensation, long-shunt compensation is also self-regulating in nature. In the same manner, analysis of long-shunt SP-SEIG along with a single mode of excitation and the series capacitor banks of 38.5 and $350\ \text{F}$ respectively, have also been computed and predicted by using the RK4 subroutine and illustrated in **Figures 5** and **6**. Here, the value of series capacitor is more than the twice of short-shunt series capacitor.

4.2.1 When both three-phase winding sets are connected in long-shunt configuration with independent R loading

The analytical waveform of voltage, current, magnetizing flux and magnetizing current during no-load and sudden switching of R load of $200\ \Omega$ at $t = 2\ \text{s}$ with long-shunt compensation along both three-phase winding sets are respectively shown in **Figure 5a, b, d** and **g**. Combined amplitude waveforms of magnetizing flux, steady-state saturated magnetizing inductance and dynamic (tangent, slope) inductance is shown in **Figure 5f**. The angular displacements of the magnetizing current space vector with respect to the d-axis of the common reference frame are also shown in **Figure 5j** and **k**. The application of the long-shunt scheme results in less overvoltage or reduced terminal voltage across the generator terminals. As it is shown in **Figure 5a**, the per phase voltage level is less than the voltage level of **Figure 3a**. It gives evidence that long-shunt SP-SEIG is able to deliver output power at reduced terminal voltages, as shown in **Figure 5c**. The combined d-q axis voltage drop across the series short-shunt capacitor is given in **Figure 5c** and combined amplitude waveform of d-axis stator current and load current during no-load and sudden switching of resistive load of $200\ \Omega$ at $t = 2\ \text{s}$ is given in **Figure 5e**. The d- and q-axis load currents are also depicted in **Figure 5h** and **i** respectively, during sudden switching of resistive load of $200\ \Omega$ at $t = 2\ \text{s}$. The steady state no-load voltage is generated at rated speed of $1000\ \text{RPM}$.

4.2.2 When both three-phase winding sets are connected in long-shunt configuration with independent R-L loading

In the same order of figure numbers, all computed waveforms are also shown in **Figure 6** with sudden switching of R-L load (200 Ω resistance in series with 500 mH inductor) at $t = 2$ s. The RMS analytical value of steady state voltage is generated at rated speed of 1000 RPM. Same like as Section 4.1, the d-q axis drops in generating and lagging load currents are also given in **Figure 6b, h** and **i**.

5. Discussion

In the machine model, two mixed state space variables have been chosen in place of single state space variable (general case). Double mixed stator current and air-gap flux state space model belongs to one of the more complex model types compared to remaining mixed variable model of stator flux linkages-stator current, rotor flux linkages-rotor current, rotor flux linkages-stator current, stator flux linkages-rotor current, air-gap flux-rotor current, magnetizing current-stator flux linkages and rotor flux linkages-magnetizing current. On the other perspective, considerably simpler than d-q axis winding current model and has simple matrix model. Short-shunt compensation results in overvoltage across the generator terminals during no-load. Whereas, long-shunt compensation gives reduced terminal voltage as compared to short-shunt compensation. In long-shunt configuration, deep saturation provides higher level of magnetizing (or stator) current against large load current at sudden switching of R (or RL) load. While, sometimes, in long-shunt compensation scheme, even reduced generated no load terminal voltage as compared to short-shunt scheme, can be capable of almost same generated total output power. In this fashion, when one moves from simple-shunt to short-shunt (or long-shunt) compensated SP-SEIG, voltage regulation has to be improved by maintaining almost similar magnitude of voltage response after load, as was in simple-shunt SP-SEIG at no-load in **Figure 5a** of Ref. [1]. Proposed saturated machine model will be applied in air-gap flux field orientation vector control strategy.

6. Conclusion

Mixed stator current and air-gap flux as a double state-space variables model preserves information about both stator and rotor parameters. A careful value selection of the combination, i.e. shunt and series capacitors may avoid the excessive voltage across the terminals of SP-SEIG during sudden switching of machine load. It is noticed that involvement of extra supplied reactive power as per self-regulating nature of short-shunt as compared to long-shunt series capacitors in each lines, retains the similar output profile of simple-shunt scheme, when machine load is suddenly switched on after few seconds. In both cases (R and R-L loading), the little bit of marked voltage drops were occurred during R-L loading compared to the R loading when variation from no load to full load.

IntechOpen

IntechOpen

Author details

Kiran Singh
Department of Electrical Engineering, Indian Institute of Technology, Roorkee,
Uttarakhand, India

*Address all correspondence to: kiransinghiitr@gmail.com

IntechOpen

© 2019 The Author(s). Licensee IntechOpen. This chapter is distributed under the terms of the Creative Commons Attribution License (<http://creativecommons.org/licenses/by/3.0>), which permits unrestricted use, distribution, and reproduction in any medium, provided the original work is properly cited. 

References

- [1] Singh K, Singh GK. Modelling and analysis of six-phase self-excited induction generator using mixed stator current and magnetizing flux as state-space variables. *Electric Power Components and Systems*. 2015;**43**: 2288-2296
- [2] Liao YW, Levi E. Modelling and simulation of a stand-alone induction generator with rotor flux oriented control. *Electric Power Systems Research*. 1998;**46**:141-152
- [3] Singh K, Singh GK. Stability assessment of isolated six-phase induction generator feeding static loads. *Turkish Journal of Electrical Engineering & Computer Sciences*. 2016;**24**:4218-4230
- [4] Krause PC. *Analysis of Electric Machinery*. New York: McGraw Hill Book Company; 1986
- [5] Khan MF, Khan MR. Generalized model for investigating the attributes of a six-phase self-excited induction generator over a three-phase variant. *International Transactions on Electrical Energy Systems*. 2018;**28**:e2600
- [6] Khan MF, Khan MR. Performance analysis of a three phase self-excited induction generator operating with short shunt and long shunt connections. *IEEE Biennial International Conference on Power and Energy Systems: Towards Sustainable Energy (PESTSE)*. 2016:1-6
- [7] Chermiti D, Abid N, Khedher A. Voltage regulation approach to a self-excited induction generator: Theoretical study and experimental validation. *International Transactions on Electrical Energy Systems*. 2017;**27**(5):e2311
- [8] Kohler Werner E, Johnson Lee W. *Elementary Differential Equations with Boundary Value Problems*. 2nd ed. Addison-Wesley; 2006